Giant Kerr Nonlinearities in Circuit Quantum Electrodynamics

Stojan Rebić,[1] Jason Twamley,[1] and Gerard J. Milburn[2]

[1]*Centre for Quantum Computer Technology, Physics Department, Macquarie University, Sydney, NSW 2109, Australia*
[2]*Centre for Quantum Computer Technology, Department of Physics, University of Queensland, St Lucia, QLD 4072, Australia*

(Received 2 February 2009; published 8 October 2009)

The very small size of optical nonlinearities places strict restrictions on the types of novel physics one can explore. This work describes how a single artificial multilevel Cooper pair box molecule, interacting with a superconducting microwave coplanar resonator, when suitably driven, can generate extremely large optical nonlinearities at microwave frequencies, with no associated absorption. We describe how the giant self-Kerr effect can be detected by measuring the second-order correlation function and quadrature squeezing spectrum.

DOI: 10.1103/PhysRevLett.103.150503 PACS numbers: 03.67.Lx, 42.50.Pq, 42.65.−k, 85.25.Cp

Introduction.—Given a sufficiently large optical nonlinearity with low quantum noise, it should be possible to generate and observe strictly quantum effects in electromagnetic fields. Examples of such effects include quadrature squeezing [1], generation of a superposition of macroscopically distinct quantum states [2], optical switching with single photons [3], and measurements of nonlocal correlations of entangled photon states [4]. So far, the successful demonstration of these effects has been limited to implementations with photons and atoms. The main obstacle for such an implementation—spontaneous emission—can be bypassed by exploiting quantum coherence effects in multilevel atoms. Such effects include coherent population trapping [5], electromagnetically induced transparency (EIT) [6], and others.

Recently, a novel system was shown to be capable of implementing basic quantum optical systems. Circuit quantum electrodynamics is an on-the-chip counterpart of cavity QED systems [7], that employs a quantized microwave mode held in a coplanar waveguide resonator (CPW) (substituting the standing-wave optical cavity) and a Cooper pair box (CPB) (instead of a two-level atom trapped in the cavity). This system offers an unprecedented level of tunability and flexibility in the implementation of the strong-coupling interaction limit. The aim of this Letter is to show that, by designing and utilizing multilevel coherent processes in "artificial superconducting atoms," circuit-QED systems can display effects completely analogous to coherent population trapping and EIT. In this Letter, we show that by designing a specific type of four-level artificial superconducting atom, and arranging for EIT in this system when coupled to the CPW, one obtains a giant-Kerr nonlinearity (Fig. 1). EIT is based on the use of dark resonance where quantum interference cancels the absorption of the probe signal. A strongly detuned fourth level provides an ac-Stark shift to the ground state $|3\rangle$, resulting in a self-Kerr nonlinearity free of spontaneous emission noise. Schmidt and Imamoğlu [8] predicted that this N scheme can give rise to several orders of magnitude enhancement in Kerr nonlinearity as compared to conventional schemes. Their prediction has been verified in a recent experiment by Kang and Zhu [9], although in a semiclassical regime. In our work, we show that due to the very strong coupling between the artificial superconducting atom and the CPW, the resulting giant-Kerr nonlinearity is predicted to be 3 to 4 orders of magnitude larger than what has been experimentally demonstrated so far. Moreover, we predict that the effect could be quite robust against dephasing. The presence of such large Kerr nonlinearities in a high-finesse cavity could result in a complete photon blockade giving an effective two-level behavior for the cavity mode [10–14] and a source of well resolved single photons. It could also be potentially adopted for use as a microwave single photon detector and to implement conditional quantum logic.

Below we show that one way to tailor the required multilevel artificial superconducting atom, giving a four-level N scheme (4 atomic levels with transitions in the shape of the letter N), is via the straightforward capacitive coupling of two CPBs. When this system is coupled to a

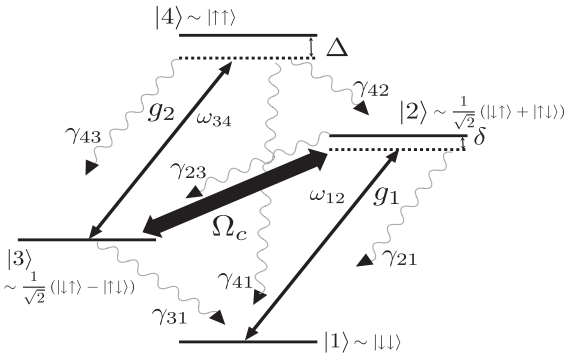

FIG. 1. N system [8], constructed from two coupled two-level CPB systems where transitions $|1\rangle \leftrightarrow |2\rangle$ and $|3\rangle \leftrightarrow |4\rangle$ are coupled with strengths g_1, g_2 to the microwave photonic mode $\hat{a}$ of frequency ω_a, held in the CPW resonator. The transition $|2\rangle \leftrightarrow |3\rangle$ is driven by the semiclassical control field Ω_c, while γ_{ij} denotes the decay rate from $|i\rangle \rightarrow |j\rangle$. We define $\Delta = \omega_{34} - \omega_a$ and $\delta = \omega_{12} - \omega_a$.

quantized CPW field, a severe photon blockade can be observed, corresponding to a huge nonlinear photon-photon interaction. The effect of quadrature squeezing is also predicted. Together, the Giant-Kerr effect of the N scheme, with the very strong coupling in circuit quantum electrodynamics (due to the large dipole moment of the CPB and the small mode volume of the CPW), gives the possibility of immensely large optical nonlinearities at the single photon level.

CPB molecule.—Normally CPBs are operated at the charge degeneracy point and act as an effective two-level system when the charging energy greatly exceeds the Josephson energy, i.e., $E_C \gg E_J$. To model a multilevel atomic system, one can capacitively couple two CPBs together to form a *CPB molecule*. For weak coupling, the CPB molecule's states $|\uparrow\downarrow\rangle$, $|\downarrow\uparrow\rangle$ are nearly degenerate, while for large coupling the corresponding eigenstates are nonperturbative superpositions of these bare states and are strongly split. This results in a formation of a multilevel system [15]. For zero detunings $\Delta = \delta = 0$, we arrange for resonance between the 34, 12 transitions and the cavity, $\omega_{34} = \omega_{12} = \omega_a$. We now show that by operating the capacitively coupled CPBs at the coresonance point, a symmetric N system is realized (see Fig. 1). With this design, we also have the important flexibility to adjust the level structure: by tuning the flux threading of the CPBs equally within the *CPB molecule*, an asymmetry is introduced leading to nonzero detunings Δ, δ.

Considering two capacitively coupled CPBs [Fig. 2(a)], the associated Hamiltonian is a combination of "Kinetic" (KE) and "Potential" (PE) terms associated with the phase difference of the wave functions across each Josephson junction $\phi_{1(2)}$. Denoting the voltage drop across the jth Josephson junction as V_j gives KE $= 1/2\sum_{j=1}^{2}(C^{(j)}V^{(j)2} + C_g^{(j)}V_g^{(j)2}) + 1/2C^{(m)}V^{(m)2}$, while the total PE $= \sum_{k=1}^{2}\mathcal{E}_J^{(k)}(1-\cos\phi^{(k)})$. $\mathcal{E}_J^{(k)}$ is the Josephson energy of the kth junction. Starting from Kirchoff's laws, we obtain

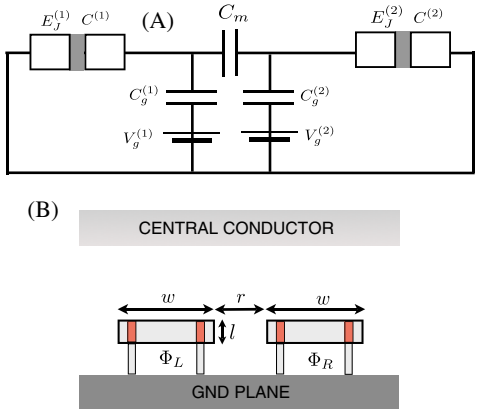

FIG. 2 (color online). (A) Circuit of two capacitively coupled CPBs with individual gate bias; (B) Schematic of possible physical arrangement of an identical ($\Phi_L = \Phi_R$) pair of CPBs to yield a *CPB molecule*.

the classical Hamiltonian

$$H = \sum_{j=1}^{2}\left(E_c^{(j)}(n^{(j)} - N_g^{(j)})^2 + \mathcal{E}_J^{(j)}(1-\cos\phi^{(j)})\right) + E_m(n^{(1)} - N_g^{(1)})(n^{(2)} - N_g^{(2)}), \quad (1)$$

where the following quantities have been defined: $\{E_C^{(j)}, E_m\} = 0.5(2e)^2\{(C_{\text{eff}}^{(j)})^{-1}, (C_{\text{eff}}^{(m)})^{-1}\}$, $\{C_{\text{eff}}^{(j)}, C_{\text{eff}}^{(m)}\} = \Xi\{(C_{\Sigma_{\{1,2\}\setminus\{j\}}})^{-1}, (C^{(m)})^{-1}\}$, $\Xi = C_{\Sigma_1}C_{\Sigma_2} - C^{(m)2}$, $C_{\Sigma_j} = C^{(m)} + C_g^{(j)} + C^{(j)}$, and where the number of excess Cooper Pairs on the gates is $N_g^{(j)} = -C_g^{(j)}V^{(j)}/(2e)$. We consider the quantized version of (1) and focus on the low energy dynamics by only including $|n^{(1)}, n^{(2)}\rangle$, $n^{(j)} = 1, 2$ states in an expansion of the Hamiltonian operator. Setting $\delta^{(j)} \equiv N_g^{(j)} - 1/2$, and denoting $\hat{Z} = |0\rangle\langle 0| - |1\rangle\langle 1|$, $\hat{X} = |0\rangle\langle 1| + |1\rangle\langle 0|$ gives

$$\hat{H}/\hbar = \sum_{j=1}^{2}(\omega_z^{(j)}\delta^{(j)}\hat{Z}^{(j)} - \omega_x^{(j)}\hat{X}^{(j)}) + J\hat{Z}^{(1)}\hat{Z}^{(2)}, \quad (2)$$

where $\hbar\omega_z^{(j)} = E_C^{(j)} + E_m/2$, $\hbar\omega_x^{(j)} = \mathcal{E}_J^{(j)}/2$, and $\hbar J = E_m/4$. If the individual CPBs are identical, then the individual Josephson energies in (2) can be modulated by local flux tuning via $\hbar\omega_x^{(j)} = E_J^{(j)} = 2\mathcal{E}_J\cos(\pi\Phi^{(j)}/\Phi_0)$. Working at the coresonance point $\delta^{(j)} = 0$, and setting $\omega_x^{(1)} = \omega_x^{(2)} = \omega_x$ yields

$$\hat{H}/\hbar = -\omega_x(\hat{X}^{(1)} + \hat{X}^{(2)}) + J\hat{Z}^{(1)}\hat{Z}^{(2)}. \quad (3)$$

The eigenenergies of (3), labeled as in Fig. 1, are $(E_4, E_2, E_3, E_1) = J \times (\epsilon, 1, -1, -\epsilon)$, where $\epsilon^2 = 1 + 4\omega_x^2/J^2$. The transition frequencies are then $\omega_{21} = \omega_{42} = J(\epsilon + 1)$ and $\omega_{23} = 2J$. To arrange for nonzero detunings $\Delta \neq \delta$ (i.e., $R \equiv \omega_{42}/\omega_{21} \neq 1$), one must move slightly off the coresonance point by introducing equal strength Zeeman terms in (2),

$$\hat{H}/\hbar = \sum_{j=1}^{2}\bar{\omega}_z^{(j)}\hat{Z}^{(j)} - \omega_x(\hat{X}^{(1)} + \hat{X}^{(2)}) + J\hat{Z}^{(1)}\hat{Z}^{(2)}, \quad (4)$$

with $\bar{\omega}_z^{(j)} = \omega_z^{(j)}\delta^{(j)}$. R can be set to any value $R \geq 1$ so adjusting $\bar{\omega}_z$ and ω_x fixes the detunings Δ, δ to any desired value without individually addressing each CPB.

To estimate the size of the coupling J, consider a closely spaced pair of CPBs as shown in Fig. 2(b) [16]. The capacitance between the two CPBs can be expressed as $C^{(m)} = 2\pi r\epsilon\epsilon_0 w/\xi$, where $\xi = K(\frac{2r}{l}) + K(\frac{2w}{l}) - K(\frac{2(w+r)}{l})$, with $K(x) = x\sinh^{-1}(1/x) + \sinh^{-1}(x)$ and $\epsilon = 9$ the relative permittivity of the substrate material [17]. We can estimate that if $(l, w, r) = (50, 10, 0.5)$ μm we obtain a large splitting: $(\omega_z^{(j)}, J) = (14.7, 2.3)$ GHz. Because of the nonlinear relationship between $C^{(m)}$ and $\hbar J = E_m/4$, the frequency $\omega_{32} \sim 2J$ for the coresonance case can be set to be MHz-GHz depending on the CPB geometry. The value $\mathcal{E}_{\text{max}}^{(1,2)} = 2\omega_x^{(1,2)} \sim 8$ GHz [7] can be reduced via adjusting the flux threading of both CPB (assuming identical CPBs

$\Phi_L = \Phi_R$). As a prototype, we choose $\omega_{43} = \omega_{21} = \omega_a = 5$ GHz, giving vanishing detunings $\Delta = \delta = 0$, if one arranges to work at the coresonance point $\delta^{(1,2)} = 0$. Then by driving the $2 \leftrightarrow 3$ transition with rf at frequency ω_{23}, one gets $J = 0.2$ GHz, and $\omega_x^{(1,2)} = E_J^{(1,2)} = 2.6$ GHz. To arrange for nonvanishing detunings, for example, we can choose to set $\omega_x/2\pi = 4$ GHz, $J/2\pi = 0.2$ GHz, $\omega_z^{(1)} = \omega_z^{(2)} = 2\pi \times 16$ GHz, and with $\kappa/2\pi = 100$ kHz, one can obtain significant differences between the transition frequencies $\bar{R} \equiv \omega_{34} - \omega_{12}$, to yield $\bar{R}/\kappa \sim 1$. One can achieve these moderate detunings even when the gate bias is offset from the precise coresonance point by a tiny amount $\delta^{(1)} = \delta^{(2)} = 2.8 \times 10^{-3}$. In the special case of identical CPBs operating exactly at the coresonance point, one has selection rules which could alter the transition strengths within our system, but as we work off coresonance we expect all transitions and decay paths to be allowed. This is a significant departure from the atomic N system studied in [8], and we will include all of these decay routes in our full model below.

Giant-Kerr nonlinearity.—It was shown [10–13] that an N system similar to one described in Fig. 1 yields an effective Kerr nonlinearity. Because of the absence of selection rules, we consider all possible decay paths with rates γ_{ij}. Drummond and Walls [18] analyzed the pure $\chi^{(3)}$ (third-order optical nonlinear susceptibility [1], Sect. 5.4), Hamiltonian $\hat{H}_{\text{eff}} = \hbar\eta\hat{a}^{\dagger 2}\hat{a}^2$ in the presence of a dissipative cavity, and using this we will estimate the size of the effective self-Kerr nonlinearity η we observe in our effective N system. For large η, the system emits photons in an antibunched manner, with large waiting times between single photon emissions. To probe these effects, the second-order correlation function $g^{(2)}(\tau) = \langle a^\dagger(t)a^\dagger(t+\tau)a(t+\tau)a(t)\rangle / \langle a^\dagger(t)a(t)\rangle^2$ will be calculated, in particular $g^{(2)}(0)$, for the weakly pumped cavity. This quantity is accepted as a good measure for photon blockade [10,12,14,19], and allows for a direct comparison with the analytical expression obtained in [18].

Before examining the combined resonator-CPB molecule in detail, we can find a rough estimate for the achievable nonlinearity η using parameters from recent optical turnstile experiments (see Table I), taking [12]

$$\eta = \left(\frac{g_1}{\Omega_c}\right)^2 \left(\frac{g_2^2\Delta}{\gamma_{43}^2 + \Delta^2} - \frac{g_1^2\delta}{(\gamma_{21}+\gamma_{23})^2 + \delta^2}\right), \quad (5)$$

which holds in the limit of $(g_1/\Omega_c)^2 \ll 1$ [11].

For the resonator-CPB-molecule system, we set $\gamma_{21} = \gamma_{23} = \gamma_{43} = \gamma = 1/T_1$, where T_1 is the lifetime of the single CPB excited state, and we take $T_1 = 10$ μs, $\kappa = 1$ MHz, and choose $(\Delta, \delta, \Omega_c) = (10, 0, 1)\gamma$. We choose the cross relaxation rates $\gamma_{42;31;41}$ to vanish (only for the purpose of this estimate) and $g_1 = g_2 = g = 300\kappa$, to obtain the enormously large Giant self-Kerr strength $\eta \approx 10 \times 10^9\kappa$. Although (5) only holds when $g_j/\Omega_C \ll 1$, this computation gives one the hint that the system (with all decay channels operational) may yield very large nonlinearities, and in the next section we model the full system to numerically verify this.

Numerical investigations.—Estimating the size of the effective nonlinearity η when $g_j > \Omega_c$ is not straightforward, as the adiabatic approximation is not permitted [10]. For that reason, we solve the master equation for the density operator ρ, given by $\dot{\rho} = \dot{\rho}_{\text{sys}} + \mathcal{L}\rho$, where

$$\begin{aligned}\dot{\rho}_{\text{sys}} = &-i\Delta_{21}[\sigma_{22}, \rho] - i\Delta_{31}[\sigma_{33}, \rho] - i\Delta_{41}[\sigma_{44}, \rho] \\ &- ig_1[a^\dagger\sigma_{12} + \sigma_{21}a, \rho] - ig_2[a^\dagger\sigma_{34} + \sigma_{43}a, \rho] \\ &- i[\Omega_c^*\sigma_{32} + \sigma_{23}\Omega_c, \rho] - iE_p[a + a^\dagger, \rho], \end{aligned} \quad (6)$$

and $\mathcal{L}\rho = \kappa\mathcal{D}[a]\rho + \sum_{(ij)}\gamma_{ij}\mathcal{D}[\sigma_{ji}]\rho$, where $\mathcal{D}[A]B \equiv 2ABA^\dagger - \{A^\dagger A, B\}$. Here, σ_{ij} describes atomic transition operators $\hat{X}^{(ij)} = \sigma_{ij} + \sigma_{ji}$ for $i \neq j$, while σ_{jj} models dephasing. $E_p \sim \sqrt{P\kappa/\omega_a}$ is the amplitude of an electric field driving the resonator mode, where P is the power of the field incident on the resonator. Summation over (ij) includes all decay channels shown in Fig. 1. We solve $\dot{\rho} = 0$ numerically to obtain $g^{(2)}(0)$. Figure 3 shows the dependence on pump strength and (classical) coupling field strength. The correlation function increases with pump strength [14]. The dependence on the coupling field shows a decrease to a minimum (solid black line) followed by an increase. This is a consequence of a nonvanishing decay γ_{31}. Increasing Ω_c pumps the population in $|1\rangle$ and diminishes the effect of decay γ_{31}, hence the decrease in $g^{(2)}(0)$. Subsequent increase with Ω_c is due to a reduction in the nonlinearity (5). Using the analytical result for $g^{(2)}(0)$ as a function of E_p/κ in [18], the effective self-Kerr nonlinearity η/κ can be deduced (shown in the inset of Fig. 3). For weak driving, effective $\eta/\kappa \sim 10^3 - 10^4$ can be obtained. As highlighted in the introduction, using this "artificial N system," optical nonlinearities of unprecedented strengths are achievable using circuit QED. This result is robust

TABLE I. Table of η from Eqn (5), measuring the size of the effective self-Kerr nonlinearity for various quantum systems coupled to cavities. We take the quoted values for (g, κ, γ), and consider additional driving (see Fig. 1) such that $(g/\Omega_c)^2 = 0.1$, [condition of validity for Eq. (5)], take $(\Delta, \delta) = (\gamma, 0)$ and $\gamma_i = \gamma$. The effective self-Kerr nonlinearity for the CPB molecule/CPW system has the potential to be extremely large. The actual model studied in this Letter contains extra decays in addition to those traditionally studied in N systems.

Work	$g/2\pi$ (MHz)	$\kappa/2\pi$ (MHz)	$\gamma/2\pi$ (MHz)	η/κ
Ref. [20]	8000	16 000	100	2
Ref. [21]	16	1.4	3	3
Ref. [22]	33	4.1	2.5	5.4
Ref. [10]	120	40	2.6	6.9
Ref. [23]				20
CPB Molecule	300	1	0.1	45 000

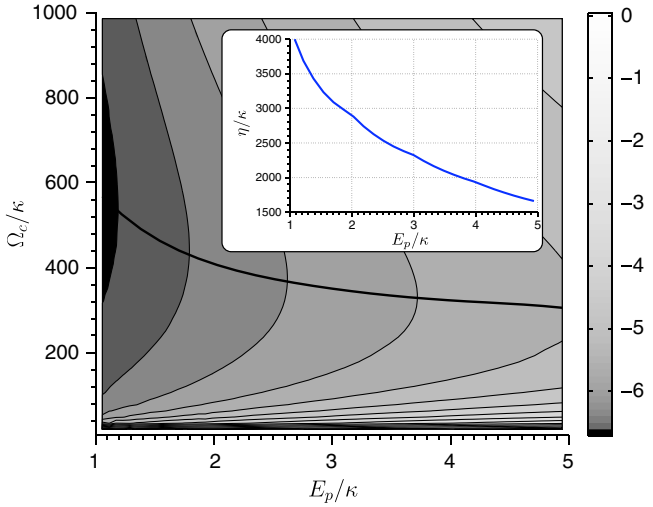

FIG. 3 (color online). Graph of $\log_{10}[g^{(2)}(0)]$ for $g = 300$, $\gamma_{23} = \gamma_{41} = 0.01$, and $\gamma_{21} = \gamma_{43} = \gamma_{31} = \gamma_{43} = 0.1$, in units of κ, and $(\Delta, \delta) = (0.5, 0.5)$. For low E_p and moderately large pumping Ω_c, the autocorrelation drops to extremely low values $\sim 10^{-6}$. The solid line indicates minimum $g^{(2)}(0)$. The inset shows the effective nonlinear coefficient η vs E_p deduced from [18], for the minimum $g^{(2)}(0)$ (see text for details). The average photon number is $\bar{n} \sim 10^{-2}$ for maximal value of the nonlinearity.

against dephasing. When we include identical rates of dephasing on all levels (taking $\gamma_{kk} = \gamma_{\rm ph} \sim 2.5\gamma_{ij}$, as seen in experiments when working off the critical point), we find that η is an order of magnitude smaller than what is shown in Fig. 3. Decreasing E_p/κ further allows one to reach values shown in the figure (and higher), and the use of transmons [24] could reduce the dephasing rate when working off the critical point.

Self-Kerr systems can produce some degree quadrature squeezing [25]. In Fig. 4, the spectrum of maximum squeezing (belonging to the amplitude quadrature) is shown. The regime where maximum squeezing is obtained

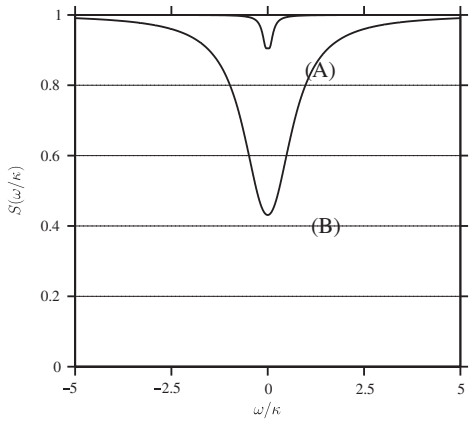

FIG. 4. Spectrum of squeezing $S(\omega/\kappa)$, for $(\Delta, \delta, g, E_p) = (5.13, -4.89, 300, 0.14)$ and (A) $\Omega_c = 50$, or (B) $\Omega_c = 1200$, and where $\gamma_{23} = \gamma_{41} = 0.01$ and $\gamma_{21} = \gamma_{43} = \gamma_{31} = \gamma_{43} = 0.1$ in units of κ.

[Fig. 4(b)] is closer to the four-wave mixing regime. Given the presence of six coherence-destroying spontaneous decay channels, the result of Fig. 4 is remarkable, since pure dispersive Kerr medium can only achieve a squeezing of $\frac{2}{3}$ [25].

While the measurement of squeezing is easy to implement using homodyne techniques, the measurement of second-order correlations involves efficient photon counters [19], which are not currently available in the microwave regime. We note, however, a recent technique [26] to obtain $g^{(2)}(0)$ by homodyne methods.

In conclusion, we have shown that an "artificial" multilevel system in circuit QED produces the effective nonlinearity orders of magnitude larger than previously known.

We acknowledge helpful discussions with T. Duty and thank the European Commission FP6 IST FET QIPC project QAP Contract No. 015848, DEST ISL Grant No. CG090188 and ARC (DP0986932) (S. R. and J. T.).

[1] D. F. Walls and G. J. Milburn, *Quantum Optics* (Springer, Berlin 2008), 2nd ed..
[2] B. Yurke and D. Stoler, Phys. Rev. Lett. **57**, 13 (1986).
[3] B. Dayan *et al.*, Science **319**, 1062 (2008).
[4] Z. Y. Ou and L. Mandel, Phys. Rev. Lett. **61**, 50 (1988).
[5] E. Arimondo, in *Progress in Optics XXXV*, edited by E. Wolf (Elsevier, Amsterdam, 1996).
[6] M. Fleischhauer, A. Imamoğlu and J. Marangos, Rev. Mod. Phys. **77**, 633 (2005).
[7] A. Blais *et al.*, Phys. Rev. A **69**, 062320 (2004).
[8] H. Schmidt and A. Imamoğlu, Opt. Lett. **21**, 1936 (1996).
[9] H. Kang and Y. Zhu, Phys. Rev. Lett. **91**, 093601 (2003).
[10] A. Imamoğlu *et al.*, Phys. Rev. Lett. **79**, 1467 (1997); P. Grangier *et al.*, *ibid.* **81**, 2833 (1998); A. Imamoğlu *et al.*, *ibid.* **81**, 2836 (1998).
[11] K. M. Gheri *et al.*, Phys. Rev. A **60**, R2673 (1999).
[12] S. Rebić *et al.*, J. Opt. B **1**, 490 (1999).
[13] M. J. Werner and A. Imamoğlu, Phys. Rev. A **61**, 011801 (1999).
[14] S. Rebić *et al.*, Phys. Rev. A **65**, 063804 (2002); **65**, 043806 (2002).
[15] A. Blais *et al.*, Phys. Rev. A **75**, 032329 (2007); M. Wallquist *et al.*, Phys. Rev. B **74**, 224506 (2006); A. D'Arrigo *et al.*, New J. Phys. **10**, 115 006 (2008).
[16] O. Gywat *et al.*, Phys. Rev. B **73**, 125336 (2006).
[17] See, e.g., M. Mariantoni *et al.*, Phys. Rev. B **78**, 104508 (2008).
[18] P. D. Drummond and D. F. Walls, J. Phys. A **13**, 725 (1980).
[19] K. Birnbaum *et al.*, Nature (London) **436**, 87 (2005).
[20] D. Englund *et al.*, Nature (London) **450**, 857 (2007).
[21] P. Maunz *et al.*, Nature (London) **428**, 50 (2004).
[22] K. M. Birnbaum *et al.*, Nature (London) **436**, 87 (2005).
[23] A. Imamoğlu *et al.*, Phys. Rev. Lett. **79**, 1467 (1997).
[24] J. Koch *et al.*, Phys. Rev. A **76**, 042319 (2007).
[25] M. J. Collett and D. F. Walls, Phys. Rev. A **32**, 2887 (1985); M. D. Reid and D. F. Walls, Phys. Rev. A **32**, 396 (1985).
[26] N. B. Grosse *et al.*, Phys. Rev. Lett. **98**, 153603 (2007).